

# On the instability of high explosive contact interface

Fedir V. Sirotkin, Jack J. Yoh  
School of Mechanical and Aerospace Engineering  
Seoul National University, Seoul, 151-742, Korea

## 1 Introduction

Turbulent mixing in fireballs is of scientific interest for variety reasons because it can lead to an afterburning of under-oxidized explosive such as TNT. The afterburning can add significant energy to the blast wave. However, amount of the energy added is difficult to estimate because it depends on the mixing rate which is not well known. The experimental study of this process is difficult due to the destructive nature of the flow, and thus computational simulations play significant role to elucidate the flow physics.

Mixing regions frequently contain jet like structures. These structures form when an explosive is mixed with the aluminum, glass, liquid (water) and mixed liquid + glass particles [1], suggesting that the chemical kinetics does not play an important role in their formation.

It was reported in experimental photography [2], that the instability of the contact interface of metalized explosives grows before solid particles cross contact interface, suggesting that instability can be responsible for the formation of jet-like structures.

Past studies of homogeneous explosive charge have identified four sequential phases to the problem [3]. These are summarized as (i) blast wave phase, (ii) implosion phase, (iii) re-shock phase, and (iv) asymptotic phase. During blast wave phase, where the mixing region is swept outward by the shock induced flow, the mixing width,  $\Delta R$ , grows linearly with time,  $\Delta R \propto t$ . This is consistent with the Richtmyer-Meshkov type instability. During implosion phase, the power-law exponent increases as a result of the inward stretching of the interface back to origin. It was found numerically that during this phase  $\Delta R \propto t^\tau$  with  $1 < \tau < 2$  [3].

The detailed study of the mixing requires numerical analysis to deal with various types of instabilities. On the other hand, the estimation of the mixing width requires accurate evaluation of the contact interface position which is hard to achieve in some cases, because the deformation of the interface can be extremely high due to the growth of instabilities.

The estimation of the mixing width requires application of the interface tracking algorithms, such as front tracking schemes. The interface conditions in these schemes impose equal pressure and equal normal velocities. Another way is the tracking of the explosive products mass fraction [3]. With this approach, the mixing width is the width along which the concentration of detonation products drops below certain level. Although such definition of the mixing layer is ad hoc, it gives the measure of the mixing layer width which is typically close to that based on interface tracking algorithms.

We investigate the stability of a rapidly expanding material interface and focus on the development of the perturbations around the contact interface by solving a two-dimensional system of partial differential equations using 2<sup>nd</sup> order Godunov Smoothing Particle Hydrodynamics (SPH) method. SPH is a gridless Lagrangian particle method [4] especially favorable in areas including free surface and interfacial flows, multi-phase flows, high-velocity impacts, penetration, shock damage in solids,

and explosion phenomena. Regarding simulations of explosions phenomena, SPH was successfully applied for underwater explosion [5], detonation of TNT charge of complex geometry [5], and detonation of heterogeneous explosives [6]. The choice of the method is justified because with SPH the mixing of the different fluids is naturally represented by means of particle motion. In particular, the layers of particles which represent, for instance, condensed (high density) explosive products and ambient air do not mix, while the boundary between them coincides with the position of the contact discontinuity. In contrast to Eulerian grid based methods, where the detection of the interface requires an application of the level set or similar interface tracking method, the Lagrangian meshless nature of the SPH allows to precisely define the position of the interface without additional computational expenses, making it suitable for instability simulation of detonation product motion.

## 2 Method

Contrary to multidimensional grid-based schemes, in SPH all interactions between the pair of particles is reduced to a one dimensional problem on the line joining them. The conservation form of the Euler Equations is

$$\frac{\partial U}{\partial t} + \frac{1}{\rho} \frac{\partial F(U)}{\partial x} = 0 \quad (1)$$

where  $U$  is the vector of conserved variables and  $F$  is the numerical flux:

$$U = \begin{bmatrix} 1/\rho \\ u \\ E \end{bmatrix}, \quad F = \begin{bmatrix} -u \\ p \\ pu \end{bmatrix} \quad (2)$$

where  $E = \epsilon + 0.5u^2$  is the specific total energy,  $\epsilon$  is the internal energy,  $p$  is the pressure,  $u$  is the velocity,  $\rho$  is the density. The set of equations (2) is closed with the equation of state  $p = (\gamma - 1)\rho\epsilon$ , where  $\gamma$  denotes the ratio of specific heats. This system has three characteristic speeds:  $-C$ ,  $0$  and  $C$ ; where  $C = c\rho$  is the Lagrangian speed,  $c$  is the sound velocity. The density is estimated from the spatial distribution of particles and their smoothing lengths as follows:

$$\rho_i = \sum m_j W(r_{ij}, h_{ij}), \quad h_{ij} = 0.5[h_i + h_j] \quad (3)$$

where  $m_j$  is the mass of the particle  $j$ ,  $h_i = k(m_i/\rho_i)^{1/\alpha}$  is the variable smoothing length,  $\alpha$  is the number of spatial dimensions,  $k$  is the parameter,  $r_{ij}$  is the distance between particles  $i$  and  $j$ ,  $W$  is the kernel function. The summation is performed over the all particles. We use quintic spline kernel [4].

Using SPH formalism the energy and momentum equations can be written as follows:

$$\begin{aligned} \frac{du_i}{dt} &= -\frac{2}{\rho_i} \sum \frac{m_j}{\rho_j} e_{ij} F_{ij} \frac{dW}{dq} \\ \frac{dE_i}{dt} &= \frac{2}{\rho_i} \sum \frac{m_j}{\rho_j} F_{ij} \frac{dW}{dq} \end{aligned} \quad (4)$$

where  $e_{ij} = |r_i - r_j|/r_{ij}$ ,  $F_{ij}$  is the flux from the solution of 1D Riemann problem between particles  $i$  and  $j$ .

To make a spatially 2<sup>nd</sup> order method we use Weighted Averaged Flux (WAF) method [7]. This method is different from the MUSCL type methods where the high-order of accuracy is obtained by data reconstruction. With the WAF method the flux is the weighted average of partial fluxes

$$F^{2nd} = w_1 F_i + w_2 F^{1st} + w_3 F_j \quad (5)$$

where  $F_i$  and  $F_j$  are partial numerical fluxes defined at  $i$  and  $j$ , weights  $w_{1,3}$  defined as

$$\begin{aligned} w_1 &= \frac{1}{2} \left[ 1 - \frac{S_i}{r_{ij}} \Delta t \right] \\ w_2 &= \frac{\Delta t}{2r_{ij}} [S_j - S_i], \quad S_i = u_i - c_i, \quad S_j = u_j + c_j \\ w_3 &= \frac{1}{2} \left[ 1 + \frac{S_j}{r_{ij}} \Delta t \right] \end{aligned} \quad (6)$$

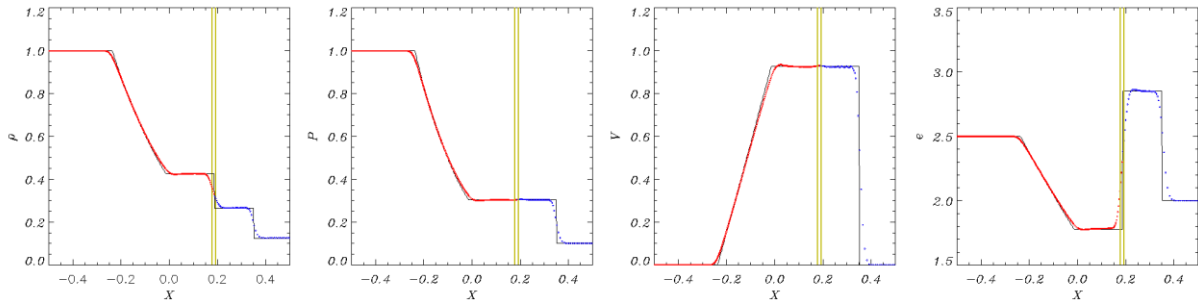


Figure 1. One-dimensional Sod's shock tube problem. Particles which are located initially to the left and to the right of contact discontinuity are illustrated with red and blue dots, respectively. The interface is located between vertical yellow lines which show the boundary where interface function drops below  $10^{-6}$ .

where  $u_i$  and  $u_j$  are projections of the velocity on  $e_{ij}$  at  $i$  and  $j$ , respectively. To solve the set of ordinary differential equations a simple predictor-corrector scheme is adopted with the time step estimated using the standard CFL conditions. The 1<sup>st</sup> order numerical flux,  $F^{1st}$ , is estimated using LLF method

$$F^{1st} = 0.5[F_i + F_j - \max(C_i, C_j)(U_j - U_i)] \quad (7)$$

In grid based methods the usual practice is to limit the contribution of the 2<sup>nd</sup> order solution using the ratio of successive gradients on the solution mesh. In the SPH this technique requires additional computational work to estimate the gradients of the integration variables at the location of the each particle. As the compromise solution we approximate the ratio of the gradients as the ratio of the primitive variables which define left and right data states of the Riemann problem as follows

$$F = F^{2nd} + F^{1st}(1 - \xi) \quad (8)$$

where flux limiter  $\xi$  is defined as

$$\xi = \beta \zeta^{1/\zeta}, \quad \zeta = \frac{\min(p_j/\rho_i, p_i/\rho_j)}{\max(p_j/\rho_i, p_i/\rho_j)}, \quad \beta = 1 - \frac{\Delta t}{r_{ij}} \max(|S_i|, |S_j|) \quad (9)$$

We found numerically that this limiter reduces the oscillations near the shock's front and contact discontinuities, while introduces moderate dissipation far from the high gradient's regions.

The position of the interface can be found tracking spatial evolution of the particles. In practice it can be achieved by assigning different colors for particles which represent different materials. Using the color we can define the "interface" function as

$$\Phi_i = \sum \frac{m_j}{\rho_j} |\omega_i - \omega_j| W(r_{ij}, h_{ij}) \quad (10)$$

where  $\omega_i$  is individual particle colors. Suppose for HE and air particles,  $\omega = 2$  and  $\omega = 1$ , respectively. Then in the area where HE and air particles are mixed,  $\Phi > 0$  while for the area where the only HE (air) particles are located,  $\Phi \approx 0$ .

We evaluate the performance of our approach in one, two and three dimensional cases with the conventional tests such as Sod shock tube. Regarding strong explosion simulations, we performed multidimensional simulations of the Sedov problem which has the analytical solution.

The result of simulation for the 1D Sod's problem is illustrated in Figure 1 with blue and red dots illustrating particles which located initially to the left and to the right of the diaphragm, respectively. The black line shows the exact solution. It can be seen, that the particles do not mix across CI, while the boundary between them coincides with the position of CI. Vertical yellow lines in the same Figure illustrate the boundaries where "interface" function drops below  $10^{-6}$ . These boundaries give the numerical width of the interface. The "numerical" width is order of the kernel width and tends to the delta function as resolution increases. With SPH the detection of the interface position is trivial task, the position of the CI interface can be found from the position of particles. Thus, with this method we do not need to apply interface tracking technique because we always know the position of the CI. The same result holds when 2D and 3D simulations are performed.

### 3 Results

The under-oxidized explosive charge is assumed to consist of TNT with a mass density of  $1630 \text{ kg/m}^3$  and a specific energy of  $4.29 \text{ MJ/kg}$ . The radius of the charge is  $R_0 = 7.36 \text{ cm}$ . The equivalent mass of the charge is  $2.4 \text{ kg}$ . The surrounding air has density of  $1.293 \text{ kg/m}^3$  and a pressure of  $1 \text{ atm}$ . Both HE products and air are treated as  $\gamma = 1.4$  ideal gases. The computational domain is a circle of  $4 \text{ m}$  radius. The charge is located at the center of the circle. The HE products and the air are represented with  $3.6 \times 10^6$  equal mass particles.

Figure 2 illustrates the temporal evolution of the CI with time. Left panels show positions of the particles with red and blue points illustrating HE and air particles, respectively. Middle panels show the contour plot of the “interface” function which gives the position of the interface. Right panels illustrate the density contour plot.

The conventional method of mixing width estimation requires computations of HE mass fraction. We divide the computational domain on  $K$  concentric layers and estimate for the each layer the area occupied by HE and air particles. The ratio of the area occupied by HE particles (red) to the total area of the circular bin gives the mass fraction of HE products,  $N_{HE}/N$ . The radial distribution of  $N_{HE}/N$  at  $t=4 \text{ ms}$  is illustrated in Figure 3.a. Using radial distribution of  $N_{HE}/N$  we defined mixing width as

$$\begin{aligned} \Delta R &= R_{max} - R_{min} \\ R_{max} &= \max(r_i) \quad i = 1 \dots K \quad N_{HE}/N > \varphi \\ R_{min} &= \min(r_i) \end{aligned} \quad (11)$$

where  $\varphi = 10^{-4}$  is the threshold,  $R_{max}$  and  $R_{min}$  give the maximal and minimal radius of the mixing zone, respectively.

Solid lines in Figure 2.b illustrate the temporal evolution of  $R_{max}$  and  $R_{min}$  in the units of the initial radius of the charge. Dotted lines in the same Figure illustrate results for the twice smaller resolution. Also the number of jets depends on the resolution (increases), the values of the radii for the given time converge when the resolution increases. It can be seen, that our simplified numerical model predicts the size of the fireball quite accurately and agrees well with results of more elaborated computations of other authors (see for instance [8])

Figure 2.c illustrates the temporal evolution of the mixing width in units of  $R_0$ . The mixing width grows nonlinearly as  $\Delta R \propto t^{1.5}$  which is again in a good agreement with previous works. However, due to parabolic deceleration of the interface the nonlinear phase starts well before implosion phase. This result is expected because we do not have initial shock within balloon model and thus the RM instability which is associated with linear regime does not develop.

Regarding metalized HE or HE mixed with solid/liquid particles, the motion of the solid particles will be strongly affected by the considered effects because motion of the gaseous and solid phase is mutually connected by the drag force (Stokes' law). The experimental results show that the jets form at the early stages of the CI development (see Fig. 4) when the effects of the afterburning do not play a significant role. Therefore, the possible explanation of the experimentally observed jet-like structures of metalized HE is the instability which occurs at the interface between explosive products and the surrounding air.

### 4 Acknowledgment

The financial support of this work was provided by ADD, Hanwha, and BK II Program through IAAT at Seoul National University.

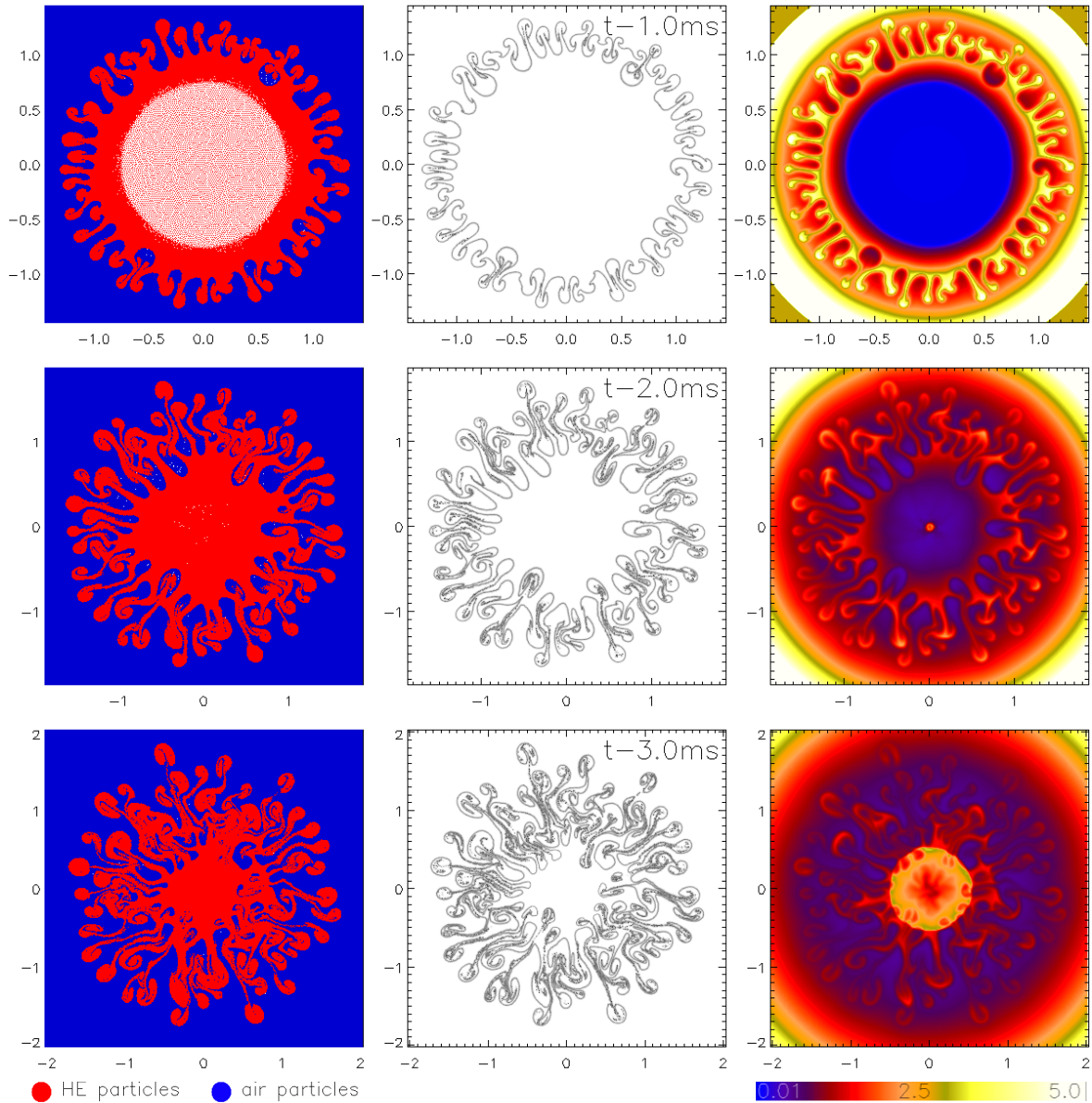


Figure 2. Positions of particles (left panels), interface position (middle) contours of density (right panels)

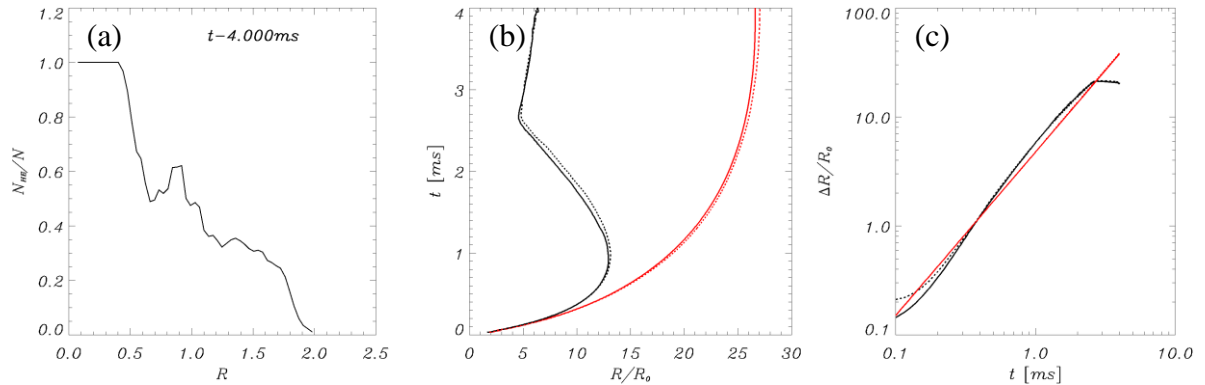


Figure 3. (a) Radial distribution of HE mass fraction, (b) temporal evolution of the maximal (red) and minimal radii (black), (c) temporal dependence of the mixing width for coarse (dotted black) and high (solid black) resolution simulations. Red line shows  $\Delta R \propto t^{1.5}$  approximation.

---

**References**

- [1] D. L. Frost, Y. Grégoire, O. Petel, S. Goroshin, and F. Zhang (2012) Particle jet formation during explosive dispersal of solid particles. *Physics of Fluids*. 24: 9
- [2] D. L. Frost, Z. Zarei, F. Zhag (2005), Instability of Combustion Products Interface from Detonation of Heterogeneous Explosives, 20<sup>th</sup> International Colloquium on the Dynamics of Explosions and Reactive Systems.
- [3] A. L. Kuhl (1996) Spherical Mixing Layers in Explosions, *Dynamics of Exothermicity*, Gordon and Breach Publishers, pp.291-320
- [4] J. J. Monaghan (2005) Smoothed particle hydrodynamics, *Rep. Prog. Phys.*, 68, 1703
- [5] G. R. Liu, M. B. Liu (2003) Smoothed Particle Hydrodynamics a meshfree particle method, World Scientific, New Jersey
- [6] A.N. Parshikov, S.A. Medin (2010) The numerical modelling of the mesostructure ow during development of the detonation in the heterogeneous explosives, [www.chemphys.edu.ru/pdf/2010-01-12-008.pdf](http://www.chemphys.edu.ru/pdf/2010-01-12-008.pdf), *Fiziko-Chimiceskaja Kinetika v Gazovoj Dinamike*, ISSN 1991-6396, 9
- [7] E.F. Toro (1989) A Weighted Average Flux Method for Hyperbolic Conservation Laws, *Proc. R. Soc. Lond.*, 423, 401-418
- [8] R. Saurel, G. Huber, G. Jourdan, E. Lapébie, and L. Munier (2012) *Phys. Fluids* 24, 115101